NEUROIMAGE **6,** 168–180 (1997)
ARTICLE NO. NI970298

Fast and Localized Event-Related Optical Signals (EROS) in the Human Occipital Cortex: Comparisons with the Visual Evoked Potential and fMRI

Gabriele Gratton,* Monica Fabiani,* Paul M. Corballis,† Donald C. Hood,† Marsha R. Goodman-Wood,* Joy Hirsch,‡ Karl Kim,‡ David Friedman,§ and Enrico Gratton¶

**Department of Psychology, University of Missouri, 210 McAlester Hall, Columbia, Missouri 65211; †Department of Psychology, Columbia University, New York, New York 10027; § Cognitive Electrophysiology Laboratory, New York State Psychiatric Institute, New York, New York 10032; ‡Functional MRI Laboratory, Memorial Sloan-Kettering Cancer Center, New York, New York 10021; and ¶Laboratory for Fluorescence Dynamics, University of Illinois, Urbana, Illinois 61801*

Received December 24, 1996

Localized evoked activity of the human cortex produces fast changes in optical properties that can be detected noninvasively (event-related optical signal, or EROS). In the present study a fast EROS response (latency ≈100 ms) elicited in the occipital cortex by visual stimuli showed spatial congruence with fMRI signals and temporal correspondence with VEPs, thus combining subcentimeter spatial localization with subsecond temporal resolution. fMRI signals were recorded from striate and extrastriate cortex. Both areas showed EROS peaks, but at different latencies after stimulation (100 and 200–300 ms, respectively). These results suggest that EROS manifests localized neuronal activity associated with information processing. The temporal resolution and spatial localization of this signal make it a promising tool for studying the time course of activity in localized brain areas and for bridging the gap between electrical and hemodynamic imaging methods.

Key Words: **noninvasive optical imaging; event-related optical signal (EROS); fMRI; VEPs; functional brain mapping; photon migration in tissues.**

INTRODUCTION

Noninvasive functional imaging of the human brain has become a central tool in neuroscience and psychology. Current procedures based on hemodynamic methods yield data with great spatial resolution and electrophysiological recordings provide excellent temporal detail (Churchland and Sejnowsky, 1988; Toga and Mazziotta, 1996). However, analysis of the time course of neural activity in specified brain areas is still difficult and often requires the adoption of modeling algorithms (e.g., Clark and Hillyard, 1996; Heinze *et al.*, 1994). In this paper we report on a novel approach to this problem based upon the use of noninvasive optical methods in combination with hemodynamic and electrophysiological data to obtain direct measures of the time course of activity in localized brain areas.

A basic premise of this approach is that neuronal activity is associated with rapid changes in optical properties of neural tissue and in particular with changes in light scattering. This is well documented in single units. Action potentials are accompanied by changes in the light scattering properties of the neuronal membrane that closely mirror the time course of the electrophysiological signal (Cohen, 1972; Hill and Keynes, 1949; Stepnowski *et al.*, 1991). Recent data support the claim that changes in light scattering can also be observed at a greater, macroscopic level: intrinsic changes in light scattering as a result of functional neural activity have been demonstrated in bloodless hippocampal slices (Frostig *et al.*, 1990) and in the exposed cortex of living animals (e.g., Malonek and Grinvald, 1996). Interestingly, Malonek and Grinvald (1996) have shown that the scattering changes begin immediately after the onset of cortical activation and return to prestimulation baseline levels immediately after the cessation of stimulation. This finding suggests that continuous measures of the scattering properties of cortical areas could be used to monitor their state of activation and therefore to provide indices of the time course of activity in these areas. The rapid time course of the scattering changes contrasts with the slower time course of the light absorption changes, which can also be observed in association with cortical stimulation. These absorption changes are related to various hemodynamic phenomena lagging the neuronal activity by up to several seconds (Frostig *et al.*, 1990; Grinvald *et al.*, 1986; Haglund *et al.*, 1992; Malonek and Grinvald, 1996; Cannestra *et al.*, 1996).

Until recently, the application of optical methods to the study of brain function was limited to measuring the activity of the exposed cortex or of very thin *in vitro* preparations (and therefore to invasive conditions, see Cannestra *et al.*, 1996; Grinvald *et al.*, 1986; Haglund *et*

1053-8119/97 $25.00

al., 1992; Frostig *et al.*, 1990). This limitation was due to two factors: (a) visible light is strongly absorbed by hemoglobin, thus reducing the penetration of the technique; and (b) head and brain tissues are highly scattering, which results in fuzzy images of deep structures. The penetration problem due to hemoglobin absorption can be partially circumvented by the use of near-infrared (NIR) light, which is only moderately absorbed by hemogloblin and can therefore travel through several centimeters of tissue. Several investigators have demonstrated that noninvasive NIR measures are sensitive to functional changes occurring in the brain (e.g., Chance *et al.*, 1993b; Hoshi and Tamura, 1993; Villringer *et al.*, 1993). These measures were taken by illuminating one or more points on the surface of the head with a continuous NIR light source and observing the amount of light reaching detectors located some centimeters distant. Measures obtained in this fashion have low spatial specificity because the photons traveling between the source and the detector through scattering media (such as the head) may follow very different paths. Therefore phenomena occurring in different locations may all influence the optical measures. Recently, however, it has been shown that it is possible to provide high-resolution images of objects immersed in scattering media using time-resolved photon migration methods (Chance, 1988; Chance *et al.*, 1993a; Delpy *et al.*, 1988; Fishkin and Gratton, 1993). The fundamental logic of these methods is that although photons diffuse (or "migrate") in a random fashion through scattering media, the time taken by photons to travel through the medium ("photon delay") is dependent on the length of the path followed by the photons in their migration. In general, photons that have traveled quickly through the medium are likely to have followed relatively homogenous paths (i.e., to have traveled through circumscribed areas of the medium). Therefore measures taken using these photons will be specific to more restricted sections of the medium. Phantom measures have demonstrated that appropriate scanning techniques based on time-resolved optical measures may be capable of detecting and localizing scattering or absorbing objects as small as 0.5 mm in diameter at a depth of several centimeters from the surface of a scattering medium (Chance *et al.*, 1993a). The resolution achievable from *in vivo* applications is not likely to be as good because of increased noise levels. Nevertheless, these data suggest that time-resolved noninvasive optical methods can, in principle, be capable of yielding fairly localized measures of brain activity.

Changes in light scattering such as those due to neuronal activity can be expected to produce small but measurable variations in the time photons take to travel through the brain (i.e., in photon delay). Previous studies (Gratton *et al.*, 1995a,b) employing time-resolved photon migration methods suggest that it may in fact be possible to detect fast and localized changes in photon delay in the brain using noninvasive measures. In particular, the data reported by Gratton *et al.* (1995a) showed that the fast optical response (termed event-related optical signal, or EROS) following a visual stimulus has a latency of approximately 100 ms. The EROS response is characterized by an increase in the time taken by near-infrared photons to travel across occipital head regions. The location of this response within the occipital region changes as a function of the area of the visual field that is stimulated in a fashion that is consistent with the known retinotopic maps of the visual field in primary visual cortex (V1, or striate cortex).

These data show that the EROS has properties that make it ideally suited to study the time course of activity in specified brain areas. In fact, its latency appears to be roughly consistent with that of the electrophysiological response recorded from the same region, and its localization is generally similar to that identified with brain imaging methods. However, a direct comparison with the time course of the electrical signal is required. Further, it needs to be shown that EROS is specific to the cortical areas that are involved in information processing. Although the data reported in previous studies do indeed show some form of spatial specificity, it is important to demonstrate that the spatial properties of the EROS correspond to those of other well-known physiological signals. Electrophysiological methods and hemodynamic imaging methods are considered the "gold standards" for temporal and spatial analyses of human brain activity, respectively (Toga and Mazziotta, 1996). The approach used in the present study is to compare EROS, functional magnetic resonance imaging (fMRI), and visual evoked potential (VEP) data obtained from the same subjects under similar stimulation conditions. The stimuli were designed to activate the upper and lower banks of the primary visual cortex (V1, or Brodmann's area 17) in each hemisphere. Area V1 has a contralateral inverted organization in humans. If EROS is a direct consequence of localized neuronal activity elicited by the presentation of the stimuli, then (a) it should be roughly localized to the same areas in which hemodynamic changes are revealed by fMRI and (b) it should have a latency similar to that of the VEP.

METHODS

Subjects. Subjects were three young adults (one female, age range 20–26), with normal or corrected-to-normal visual acuity of 20/20 or better. Subjects gave written informed consent. Two of the subjects (PC and MG, a male and a female) were run in 12 sessions in which optical measures were recorded from different

locations, 1 session in which VEPs were recorded, and 1 session in which an fMRI was recorded. The third subject (JG) was run only in the optical and VEP sessions.

Stimuli. For all types of measurements, the four quadrants of the visual field were stimulated on different trials. For the optical and VEP sessions, stimuli were reversals of one of four vertical black-and-white grids (size: ≈4° horizontally and ≈6.5° vertically, eccentricity ≈7°, spatial frequency ≈4 bars per degree) occurring every 500 ms during stimulation periods lasting 19 s. Stimulation periods were separated by rest periods with a duration of approximately 20 s. In each session, there were a total of 48 stimulation periods (12 for each quadrant of the visual field), yielding a total of 456 reversals (trials) for each stimulation condition. For the fMRI session, stimuli were flashes (frequency ≈4 Hz) of vertical black-and-white grids that were located in the same locations and of sizes similar to those described above. The fMRI session consisted of eight 30-s stimulation periods alternated with rest periods.

Optical recordings. The optical measurements involved placing a device consisting of a near-infrared light source (light emitting diode, or LED, wavelength 715 nm, power 200 μW) and a detector (a 0.64-cm-diameter optic fiber connected to a photomultiplier tube) over the scalp on 12 locations (1 per session) in the occipital area. A source–detector distance of 3 cm was selected to obtain a depth of measurement ranging between 1.5 and 3 cm (see Gratton *et al.*, 1995b). Measurements of photon delay were based on frequency domain methods (Gratton and Limkeman, 1983). Photon delay was measured with a frequency domain spectrometer (Gratton *et al.*, 1984) using a light source modulated at a frequency of 112 MHz and a cross-correlation frequency of 1 kHz. The average photon delay was computed over intervals of 50 ms. The recording of the optical parameters is completely noninvasive since the electromagnetic radiation used is non-ionizing and of very low intensity (less than 1 mW). In addition, the skin is not lesioned nor abraded. In order to improve the contact between the source and detector and the skin, hairs were combed away from the recording locations before the measurements were taken.

The pulse artifact was compensated for according to a procedure described by Gratton and Corballis (1995). The individual trial data were segmented and averaged separately for each subject, condition, and location (i.e., session). Previous analyses reported by Gratton *et al.* (1995a) indicate that the photon-delay signal revealed an EROS peak response at a latency of 100 ms from stimulation. Statistical analysis of the spatial distribution of this peak showed significant effects of stimulation conditions that mirrored the expected contralateral and inverted representation of the visual field in primary visual cortex (area V1). Gratton *et al.* also reported longer latency effects with a time course of several seconds, likely corresponding to hemodynamic phenomena. Other authors have reported slow changes in photon migration parameters from occipital areas due to changes in the concentration of oxy- and deoxyhemoglobin as a result of visual stimulation (Hoshi and Tamura, 1993; Kato *et al.*, 1993; Meek *et al.*, 1995). These slow effects will not be discussed further in this paper.

fMRI recordings. fMRI data were acquired on a 1.5-T magnetic resonance scanner (General Electric), retrofitted for echoplanar imaging (Advanced NMR Intrascan) and located in the Department of Radiology at Memorial Sloan-Kettering Cancer Center (see Hirsch *et al.*, 1995). T2*-weighted images were acquired using a gradient echo sequence (echo time = 60 ms; repetition time = 3 s; flip angle = 30°) and a 12.5-cm-diameter surface coil centered on the occipital pole. The in-plane resolution was 1.56 × 1.56 mm (128 × 256 matrix; 20 × 40 cm field of view). The slice thickness was 3 mm. Sixteen coronal slices were acquired, parallel to the occipital bone above the inion (these planes were selected on the basis of a midsagittal T1 image). Ten images were collected during a 30-s rest period before stimulation, 10 images were collected during the stimulation period (30 s), and 10 images were collected during a 30-s recovery period. Prior to statistical analysis, all brain images for each subject were aligned, and a two-dimensional in-plane Gaussian filter was applied to each image. Each voxel therefore represents a centroid of activation. The statistical analysis involved: (1) comparison of mean baseline and stimulation signals, (2) comparison of mean stimulation and recovery baseline signals, and (3) coincidence analysis by comparison of activation on two independent runs. The empirical probability of passing all three stages of the analysis by chance was determined from images acquired from a "phantom" (using the General Electric standard). Using this procedure, the rate of false positives was determined to be ≤0.0001 for the pixels indicated in red in Fig. 1 and smaller for the pixels indicated in orange and yellow (with yellow corresponding to the minimum probability of a false positive).

VEP recordings. VEPs were recorded using a sampling rate of 200 Hz (bandpass = 1–100 Hz) from an array of 22 electrodes for a period of 400 ms beginning with stimulus onset (i.e., with each grid reversal). The initial value of the recording epoch was used as baseline. The impedance was kept below 10 kOhm. The electrode montage was derived from that used by Spekreijse and collaborators in their work on modeling the sources of visual evoked potentials (e.g., Maier *et al.*, 1987). The montage consisted of four horizontal rows covering the back of the head. The highest and

lowest rows comprised four electrodes, whereas the two middle rows comprised seven electrodes. The interelectrode distance was 4 cm for both the vertical and the horizontal axes. The bottom row was located 2 cm below the inion, and the array was symmetric with respect to the midline. A frontal electrode was used as reference. There were 456 trials per condition. The electrophysiological recordings included bipolar vertical and horizontal EOG derivations (from above and below the right eye, respectively, and from locations 2 cm external to the outer canthi of each eye) that were used for off-line correction of the ocular artifact (Gratton *et al.,* 1983). The average VEP was computed separately for each subject, electrode location, and stimulation condition.

Coregistration. The estimates of the foci of optical, fMRI, and VEP activities were aligned using scalp and skull landmarks (e.g., inion, ear canals, nasion). For the optical and VEP data, the alignment was based on the localization of the inion, which was used as a reference location for both techniques. The T2*-weighted fMRI data were aligned with those obtained with the other techniques on the basis of the localization of ear canals, inion, and nasion on the T1-MRI images.

RESULTS

Time course of optical activity. The purpose of this analysis was to examine the time course of the optical activity, and, in particular, to determine the latency of the first detectable EROS peak in response to individual grid reversals. Because of the well-known intersubject variability in the anatomy of the occipital cortex, it is critical to determine which of the 12 optical recording locations should be used to characterize the time course of the optical activity. One way to approach this problem is to identify the recording locations corresponding to the surface projections of the maximum fMRI activity for each subject and condition and then average the time course of optical activity recorded in these locations. The fMRI data were obtained for two subjects in each of the four conditions. The fMRI maps shown in Fig. 1 reveal multiple areas of significant activity. Note that only the slice with maximum BOLD-fMRI activity is shown in the figure, although for each condition and subject 12 fMRI slices were obtained.

Significant fMRI activity occurred in both medial (i.e., proximal to the calcarine fissure) and lateral occipital areas. The medial areas are likely to reflect activity within area 17 (primary visual cortex), while the more lateral areas are likely to represent activity within extrastriate visual areas. An interesting aspect of these data (visible from an inspection of Fig. 1) is that, whereas the location of the medial fMRI activity varied systematically as a function of the experimental conditions (i.e., it was located in the contralateral hemisphere and in higher areas for stimulation of lower quadrants than for stimulation of upper quadrants), the location of the lateral fMRI activity did not appear to vary as a function of the stimulated quadrant.

An example of the time course of EROS is shown in Fig. 2. This figure shows maps of EROS obtained at different latencies for the upper left stimulation condition of subject PC. For comparison purposes, these maps are presented using the same left–right radiological convention used for fMRI. The area depicted in Fig. 2 corresponds to the large rectangles superimposed on the fMRI images presented in Fig. 1 (upper left condition of subject PC). When compared to the corresponding fMRI map, this figure indicates that the medial (right hemisphere) and lateral (left hemisphere) areas showing activity in the fMRI maps also show EROS activity. In addition, EROS shows that the activities in the medial and lateral areas differ in their respective time courses. The medial area shows a maximum increase in the phase delay parameter at a latency of 100 ms after stimulation, whereas the lateral area shows a maximum at a latency of approximately 200 ms. For both areas, activity declines at longer latencies.

In order to determine the generality of this phenomenon, for each subject and condition, two optical recording locations were selected: the first corresponded to the location of the medial fMRI activity (i.e., presumably activity from area 17) and the second corresponded to the location of the lateral fMRI activity (presumably activity in lateral occipital areas). The time courses of the optical activity recorded in medial and lateral areas were then averaged separately across subjects and conditions. The EROS time course waveforms corresponding to the medial and lateral areas of fMRI activity are shown in Fig. 3. Note that in this figure the EROS peak latency for lateral areas of fMRI activity was 300 ms, somewhat longer that indicated in Fig. 2 (in which data from only one subject and condition were presented). The average activity from all other optical recording locations, corresponding to areas in which no significant fMRI activity was observed, is also shown in this figure.

These waveforms indicate that the EROS from the recording locations corresponding to the areas identified by fMRI as area 17 (or V1) peaks at a latency of approximately 100 ms (as a reminder, the optical data were sampled every 50 ms). The value of phase delay observed at this latency was significantly greater than that observed during the prestimulus baseline period, $t(7) = 4.85$, $P < 0.005$ (two-tailed).[1] Note that this result is still significant at an $\alpha < 0.05$ level if the

[1] There were a total of eight comparisons between fMRI and optical data sets in the study (four conditions for each of two subjects).

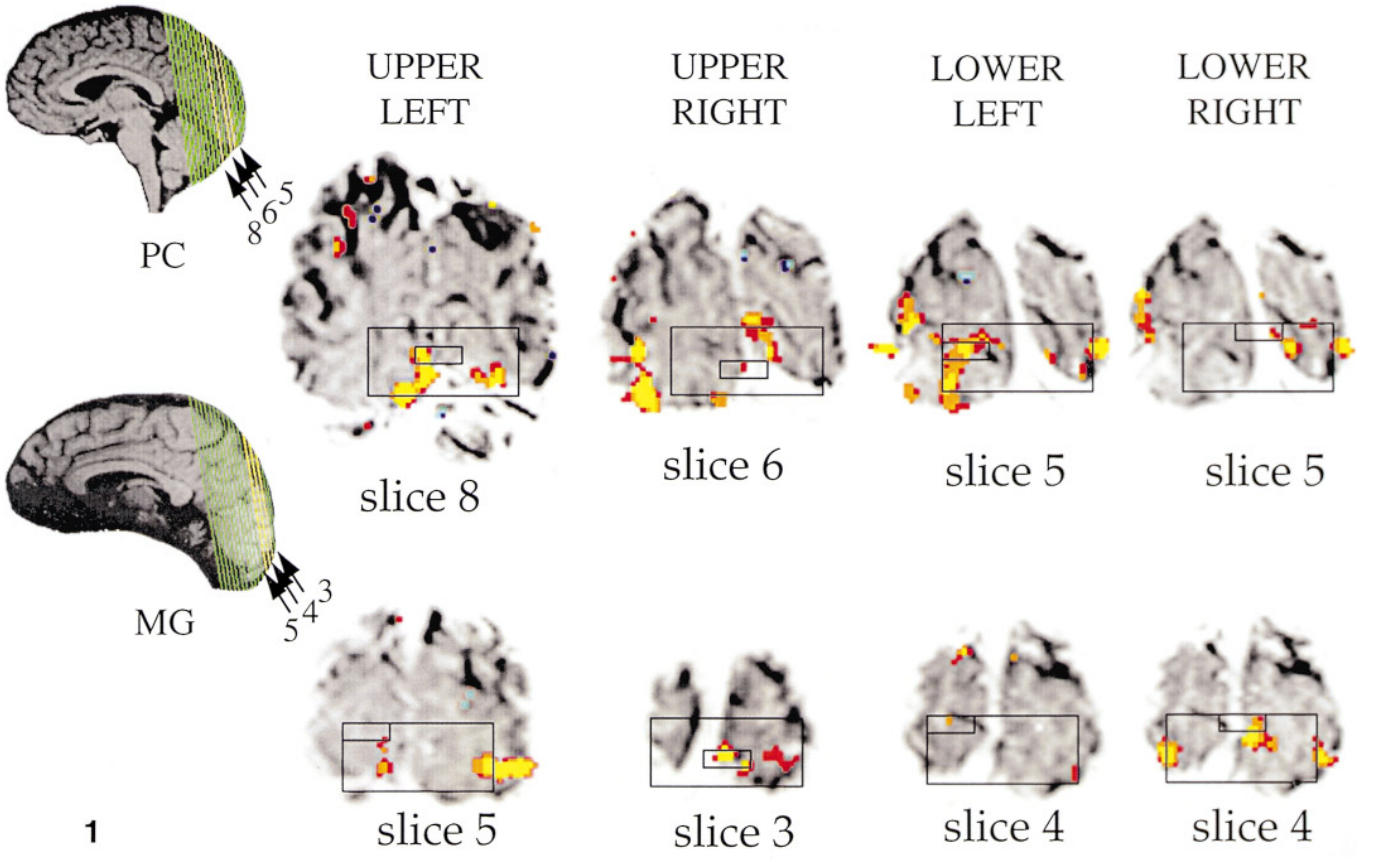

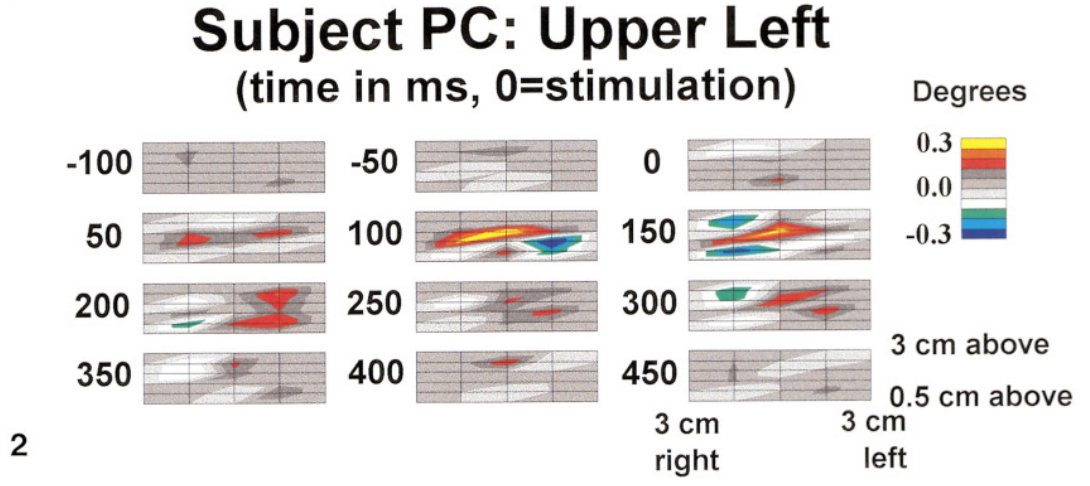

FIG. 1. The fMRI responses (yellow, red, orange) and optical responses (small rectangles) are superimposed on these images. The locations of the brain sections shown in the figure are indicated in yellow on the midsagittal T1 images presented to the left. For each subject and condition, the slice containing the maximal increase in the fMRI signal during the 30-s stimulation period (with respect to the rest period) was selected and is indicated by slice number at the bottom of each image. In this study the focus is on medial regions of the brain, presumably Brodmann's area 17 (primary visual cortex), as opposed to lateral regions, which are presumably areas further along the visual pathway. In each map, the cortical area explored with EROS measures is represented by the large rectangle, whereas the small rectangle represents the EROS recording location with maximal response (i.e., maximal increase in photon delay at a latency of 100 ms after each grid reversal). EROS and fMRI images were aligned using skull landmarks (e.g., inion, ear canals). Images are displayed according to the standard radiological convention (i.e., the left hemisphere is presented to the right).

FIG. 2. Example of the time course of the EROS from one subject (PC) and one stimulation condition (upper left). Each map represents the activity at a particular data point from 100 ms before stimulation (i.e., grid reversal) to 450 ms after stimulation. The time at which the maps were taken is indicated to the left of each map. The color scale used for map construction is shown to the right. The coordinates of the area mapped are shown on the last map, with reference to the position of the inion (typically the primary visual area—area 17 or V1—is located approximately 2 cm above the inion, within 2 cm from the midline). The 12 recording locations correspond to the intersection of the vertical and horizontal lines reported in each map. The inverted left–right radiological convention is used in this figure to facilitate comparison with the fMRI maps shown in Fig. 1.

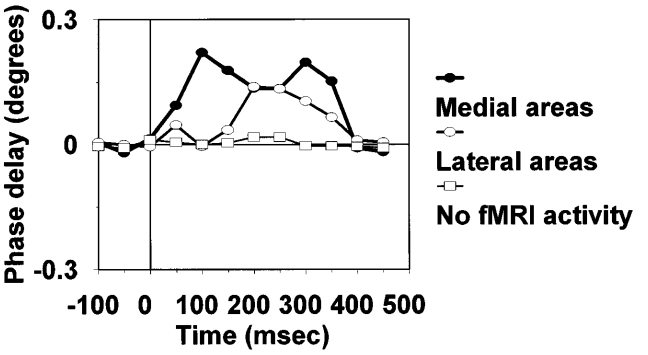

FIG. 3. Time course of the EROS averaged across subjects and stimulation conditions for optical recording locations corresponding to medial (area 17 or V1) regions of fMRI activity (black circles), lateral (extrastriate) regions of fMRI activity (open circles), and regions in which no significant fMRI activity was observed (open squares). Time is expressed in ms with 0 indicating the time of stimulation (grid reversals). EROS activity is expressed in degrees of phase with respect to a prestimulus baseline (average of 100 ms before stimulation).

Bonferroni inequality is applied for multiple comparisons at all possible poststimulus latencies ($\alpha < 0.00625$). Note also that the optical activity was already significant at a latency of 50 ms and remained significant until a latency of 350 ms (for all latencies, $t(7) \geq 2.49$, $P < 0.05$).

The time course of EROS in the lateral locations identified with fMRI was quite different, peaking between 200 and 350 ms after stimulation. This activity was also of lesser amplitude. Separate comparisons for each latency bin with the baseline value revealed a significant difference at all latencies between 200 and 350 ms ($t(7) \geq 3.08$, $P < 0.05$). No significant EROS activity was observed from locations corresponding to areas in which no fMRI activity was observed.

Overall, these data indicate that (a) an EROS peak with a latency of 100 ms can be observed in primary visual cortex (area 17, or V1), (b) the EROS response is generally limited to areas showing fMRI activity, and (c) EROS can be used to distinguish the time course of activity in areas where a significant fMRI response is observed (since the medial and lateral fMRI areas show peaks of optical activity occurring at different times).

Spatial congruence of EROS, fMRI, and VEP data. The spatial congruence among techniques was evaluated only for the subjects for whom fMRI data were available (subjects PC and MG). In all cases, the spatial congruence was evaluated with respect to activity that was deemed to occur in area 17 (primary visual cortex, V1). In other words, the focus was on the medial fMRI response and on the early optical response (i.e., latency = 100 ms). In order to provide independent, focal location estimates of the fMRI and EROS responses, the location of the EROS response was identified as the center of the pixel with the largest response (i.e., increase in photon delay) at a latency of 100 ms. For the fMRI, the location of the activity was identified with the geometric center of the volume in which a significant response was obtained.

TABLE 1

Coordinates of the Estimated Foci of Activity in Area 17 (V1) Obtained with the Different Procedures Used in the Study (in cm, Referred to the Inion)

		Subject PC			Subject MG		
Condition	Measure	Hor.	Vert.	Depth	Hor.	Vert.	Depth
Upper left	VEP	1.4	1.1	4.5	2.5	2.3	4.4
	EROS	0.0	2.0	<3.0	1.5	2.5	<3.0
	fMRI	0.7	1.6	2.3	1.1	1.5	2.5
Upper right	VEP	0.0	3.9	3.3	−0.7	2.3	3.5
	EROS	0.0	1.5	<3.0	0.0	1.5	<3.0
	fMRI	−0.7	2.1	2.9	0.0	1.5	1.9
Lower left	VEP	1.7	1.0	4.1	0.2	0.4	2.5
	EROS	1.5	2.0	<3.0	1.5	2.5	<3.0
	fMRI	1.8	2.1	2.0	1.5	2.5	2.2
Lower right	VEP	−0.7	3.9	5.0	−1.2	3.9	3.9
	EROS	0.0	2.5	<3.0	0.0	2.5	<3.0
	fMRI	−0.9	2.1	2.0	−0.2	2.3	2.2

Note. Hor., horizontal axis (left, negative; right, positive); Vert., vertical axis (above inion, positive; below inion, negative); Depth, distance from surface of the head. For EROS data, only the maximum acceptable depth is given.

The estimated coordinates of the location of the response obtained with each technique for each experimental condition and subject are shown in Table 1 (expressed as distances from the inion). The average distance along the vertical and the horizontal axes between the estimated foci for each technique is reported in Table 2 (the distance along the depth axis is not included because the EROS data provide only range values for this axis). The average distances calculated over the vertical plane formed by the horizontal and vertical axes are also reported in this table.

A graphic representation of the relative localization of EROS and fMRI signals is presented in Fig. 1. This

TABLE 2

Average Distance between Estimates of Focus of Activity in Area 17 Obtained with the Different Procedures Used in the Study (in cm)

Pair of measures	Subject PC			Subject MG		
	Hor.	Vert.	Overall	Hor.	Vert.	Overall
VEP–EROS	0.6	1.4	1.6	1.0	1.1	1.6
VEP–fMRI	0.4	1.4	1.6	1.0	1.0	1.4
EROS–fMRI	0.6	0.3	0.7	0.3	0.2	0.4

Note. Hor., horizontal axis; Vert., vertical axis; Overall, distance over the vertical plane identified by the vertical and horizontal axes and roughly parallel to the surface of the head at the inion.

figure shows the fMRI tomographic slices where the maximum activation response was observed (note that the depth of the slices changed with stimulation condition and subject). The large rectangles superimposed on the images indicate the area explored with optical measures, and the small rectangles indicate the recording location at which the EROS response was maximal for each condition and subject. The average distance between the foci of EROS and fMRI activity was 0.5 cm (0.3 cm along the vertical axis and 0.4 cm along the horizontal axis). These distances were smaller than the spatial sampling error for the optical recordings (0.5 cm along the vertical axis and 1.5 cm along the horizontal axis).

We performed two additional tests to evaluate the statistical significance of the spatial relationship between EROS and fMRI foci. The rationale for the first test was that, although the data presented thus far suggest that the foci of the EROS activity are relatively close to the foci of the fMRI activity, it is important to show that they are closer than points taken at random within the area explored by the optical recordings. In other words, it is important to demonstrate that they provide specific information about the locus of the brain response as a function of stimulation within the cortical area explored. Therefore, we compared the distance between the foci of fMRI and EROS responses with the average distance between the focus of the fMRI response and the individual locations used for the optical recordings. This average distance is the expected value of the distance between EROS and fMRI maxima of activity for the case in which the optical maxima reflect only random fluctuations of the phase delay value. Across subjects and conditions, the average distance between the focus of fMRI activity and all the locations used for the optical recordings ranged between 1.2 and 1.9 cm (mean = 1.5 cm). As can be seen from Tables 1 and 2, the distance between the optical and fMRI foci ranged between 0.0 and 1.0 cm. This indicates that the localization of the optical response was significantly better than chance. This was confirmed by a paired t test comparing the obtained distance between the EROS maximum and the fMRI maximum with the expected value for this distance according to the null hypothesis of random localization of optical activity ($t(7) = -5.10$, $P < 0.001$, one-tailed).[2]

The second test was based on computing correlations between the locations of the foci of optical and fMRI responses along the horizontal and the vertical axes (in each case the correlation was based on eight values). The purpose of this test was to provide a statistical index of the validity of the optical measurements. The Pearson product-moment correlation was equal to 0.87 along the horizontal axis and to 0.38 along the vertical axis. Note that the average distance between measurements for the vertical and the horizontal dimensions is relatively similar (and actually somewhat smaller for the vertical dimension). The large difference in the correlation coefficients in the two dimensions should be attributed to the fact that the experimental manipulations induced a larger variance along the horizontal dimension than along the vertical dimension. According to the design of the experiment, variance along the horizontal dimension (i.e., across hemispheres) is induced by stimulation of quadrants contained in opposite hemifields, whereas variance along the vertical dimension is induced by stimulation of the upper and lower quadrants. Stimulation of the contralateral hemifields resulted in an average separation of the foci of activation in the left and right hemispheres of 1.7 cm using fMRI estimates and 1.1 cm using optical estimates; stimulation of upper portions of the visual field resulted in foci of activity that were located 0.5 cm below those obtained for stimulation of the lower portions of the visual field (this separation was the same for estimates using fMRI and EROS). Alternatively, the difference in the correlation might be due to differences in the physiological phenomena underlying the fMRI and EROS signals.

The analyses presented so far were all related to surface projections of the cortical activity measured with fMRI and optical recordings. Surface projections were used because the optical recordings do not provide information about the depth of the effects recorded. However, a range for the expected depth of the cortical area explored using optical methods can be estimated on the basis of Monte Carlo simulations (see Gratton *et al.,* 1995b). For the conditions of the present experiment, the expected depth range is less than 3.0 cm (i.e., less than the source–detector distance). Note that the depth of the fMRI sources from the surface of the head ranged between 1.5 and 2.9 cm. Therefore, the fMRI focus was always within the range explored by EROS. However, since the optical signal presumably weakens with depth, the depth of the cortical activity may influence the accuracy of the optical localization. Indeed, the distance between the EROS and fMRI foci was positively correlated with the depth of the fMRI focus ($r = 0.55$, $P < 0.10$, one-tailed), although the correlation was not significant given the small sample size. The distance between EROS and fMRI foci was 0.3 cm for depth of fMRI foci less than or equal to the median (2.2 cm) split and 0.6 cm for depth of fMRI foci greater than or equal to the median.

Overall, the data presented in this section indicate convergence between the localization of foci of activity obtained with optical and fMRI methods within the

[2] A one-tailed test was used because the only meaningful hypothesis to be tested was whether the distance between the EROS and the fMRI activity was significantly smaller than that obtained by randomly sampling one of the optical locations.

sampling error of optical data. This convergence is particularly good for superficial sources. Thus, the data provide a validation of the localization of activity obtained with noninvasive optical methods.

Whereas optical and fMRI data refer to localized activity, the surface VEP data refer to volume-conducted activity at the surface of the scalp (grand-average VEP responses from two electrodes are shown in Fig. 4). Therefore, the VEP data were analyzed using a spatiotemporal dipole modeling approach (BESA program, see Scherg *et al.*, 1989). In this approach, the variance over scalp locations across the entire recording epoch is accounted for by a limited set of dipoles, with fixed location and orientation but with variable amplitude and polarity. In agreement with the fMRI results, we assumed that the surface VEP activity would result from the summation of activity from striate and extrastriate cortex. Therefore, a two-dipole model (with no constraints) was fitted separately to the surface VEP data recorded for each experimental condition and subject. The two-dipole model accounted, on average, for 69.0% of the variance (range 78.2–54.2%). Of the two dipoles, the one whose location was closer to the expected location of area 17 was selected as an estimate of the activity in this cortical area. The BESA algorithm estimates not only the location but also the time course of each dipole source. This approach represents a mathematical model of the observed activity and is therefore quite distinct from the empirical observation of local effects obtained with the EROS and fMRI methods. Nevertheless, source analysis represents the most appropriate procedure currently available for comparing VEP data with the other localized data sets.

The dipole analysis used in the present experiment yields a model of the localization and time course of the activity underlying the surface VEP. However, the localization of the source of VEP activity in our study was not entirely consistent with those of EROS and fMRI activity. The source-analysis algorithm separated activation of the left and right hemispheres (by approximately 2.1 cm) in the predicted manner: a contralateral dipole was observed for each condition and subject. However, the predicted top–bottom difference was not observed: the dipoles associated with stimulation of the upper quadrants were located, on average, slightly above (by 0.1 cm) those for stimulation of the lower quadrants. Further, the average distance between the surface projections of the foci of VEP and EROS activity was 1.6 cm; the average distance between the foci of VEP and fMRI activity was 1.5 cm. The distance between the surface projections of the VEP and fMRI foci was consistently larger than the distance between the EROS and the fMRI sources (by approximately 1.0 cm), $t(7) = 5.10$, $P < 0.01$ (two-tailed). Interestingly, the discrepancy between the surface projections of VEP and fMRI foci was positively correlated with the depth of the fMRI source ($r = 0.81$, $P < 0.05$, one-tailed), as it

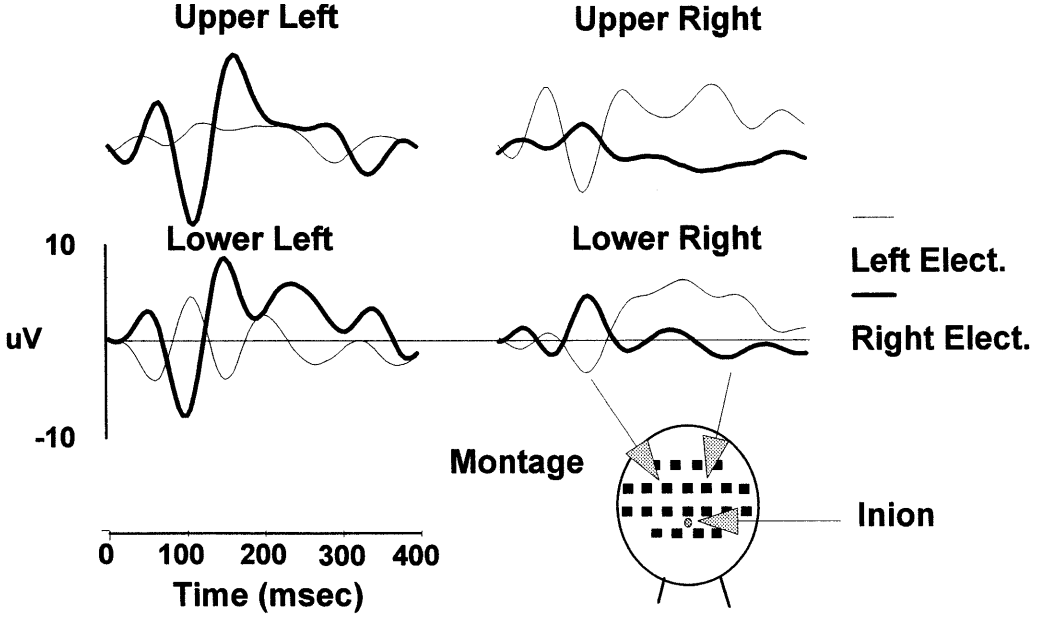

FIG. 4. Grand average VEPs ($n = 3$) for each of the four stimulation conditions from two electrode locations on the left (thin lines) and right (thick lines) of the midline. These electrode locations were selected because they showed the largest responses. The electrode montage used in the study is shown in the head diagram (back view) shown at the bottom right corner of the figure. The arrows indicate the electrode locations of the grand average waveforms displayed in the figure, as well as the position of the inion. Time is expressed in ms with 0 indicating the time of stimulation (grid reversals). The electrical activity is expressed in microvolts (positive values are plotted up) with respect to a 50-ms prestimulus baseline.

had also occurred for the discrepancy between EROS and fMRI foci. The discrepancy averaged 1.1 cm for superficial fMRI activity (less than 2 cm deep) and 1.7 cm for deeper activity. This finding suggests that dipole localization methods of the type used in the present study may be more accurate at localizing superficial activity than deep activity. In general, however, the localization was much less precise than that obtained using EROS.

Dipole localization methods also provide estimates of the depth of the VEP sources. However, in the present study large discrepancies between VEP dipole sources and fMRI activity were observed for the depth dimension. In particular, the dipole analysis procedure estimated sources of VEP activity that were systematically deeper than the foci of fMRI activity (on average, 3.9 cm vs 2.2 cm), $t(7) = 5.14$, $P < 0.01$.

Temporal congruence between EROS and VEP data. Analysis of the temporal congruence between measures could be conducted only for EROS and VEP data, since the fMRI responses (which took several seconds to reach their peaks) were too slow to assess the latency of responses to individual grid reversals. Since EROS and VEP data were obtained for all three subjects, they were all included in the analysis. A problem with comparing these two time courses is that EROS measures reflect changes in optical properties in localized areas of the head, whereas the VEP measures reflect electrical activity that is volume conducted to the surface in a manner that depends not only on the conductive properties of the medium, but also on the location and orientation of the underlying dipoles. Therefore, it is not obvious which particular electrode location should be compared with a particular optical recording location. A further problem is that there is no a priori knowledge about the relationship between the polarity of the electrical activity and that of the optical signal.

To address these problems, we used two different approaches. One approaches was based on the idea that neural activity elicited in the occipital area by visual stimuli should produce electric fields with strong local gradients and therefore should increase the variance among the recording electrodes placed above the posterior part of the head. It should also produce increased optical activity in the same area. According to this hypothesis, periods of increased EROS activity should roughly correspond with periods of increased interelectrode variability. The time course of the interelectrode variability (i.e., the standard deviation across electrode locations), averaged across subjects and conditions, is shown in Fig. 5.[3] These data show that increases in interelectrode variability are observed at a latency of approximately 100 ms and, later on, at a latency of approximately 250 ms after stimulation. Note that these two latency periods correspond to the epochs in which increases in optical activity are observed within and outside of area 17 respectively, (cf. Fig. 3).[4] In order to determine whether this correspondence is more than coincidental, we estimated the latency of the maximum variability within the first 130 ms after stimulation for each subject and condition. We then compared this estimate with the latency of the EROS peak (defined as the largest increase in phase delay within the first 150 ms after stimulus across all optical recording locations).[5] These values are reported in Table 3.

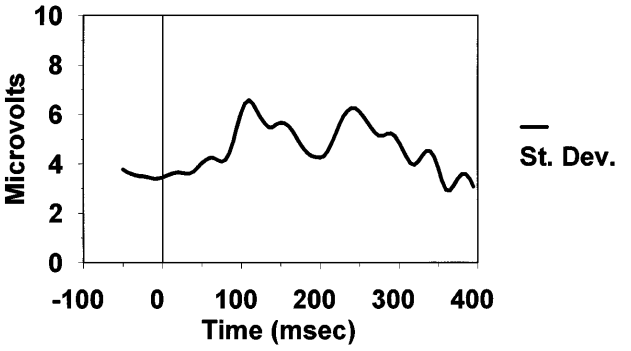

FIG. 5. Time course of the interelectrode variability (standard deviation across electrodes) of the visual evoked potential, averaged across subjects and stimulation conditions. Time is expressed in ms with 0 indicating the time of stimulation (grid reversal). The interelectrode standard deviation is expressed in microvolts. Note that no baseline value was subtracted from the data in order to avoid biasing the shape of the interelectrode variability waveform.

The values reported in this table indicate the existence of correspondence between the latency of the peak of optical activity and that of the interelectrode variability. The product-moment correlation coefficient between these two sets of values is significant ($r = 0.74$, $P < 0.01$).[6] The average absolute difference in the la-

[3] If a prestimulus baseline value was subtracted from the average waveforms obtained at each electrode, the interelectrode standard deviation during the prestimulus baseline period would likely be smaller than that after stimulation. Therefore, the baseline value was not subtracted from the evoked potential data used to compute the standard deviation values displayed in Fig. 5 in order to obtain stationary conditions that would not bias the standard deviation estimates, making them larger in one part of the recording epoch with respect to another.

[4] An alternative explanation for the difference in the latencies of the EROS responses in medial and lateral occipital areas might be that there are differences in the latency of scattering (or absorption) phenomena rather than differences in the latency of neuronal activity.

[5] The window was somewhat shorter for the VEP than for the EROS data because (a) they were collected using a higher sampling rate (200 Hz vs 20 Hz) and (b) it was important to make sure that the VEP variability peak corresponded to the first peak of activity observed.

[6] Note that the observations obtained for each subject and condition that have been used for the computation of this correlation are not independent, which may increase the probability of α error. To

TABLE 3

Estimates of the Latency (in ms after Stimulation) of EROS and VEP Activity for Each Subject and Stimulation Condition

Latency measure	Subject	Upper left	Upper right	Lower left	Lower right	Average
VEP: Peak of inter-electrode variability (ms)	PC	105	115	120	130	117
	MG	115	70	105	125	104
	JG	95	40	65	85	71
	Average	105	75	97	113	97
EROS: Peak of phase delay increase (ms)	PC	100	100	150	100	113
	MG	100	50	150	100	100
	JG	100	50	50	50	63
	Average	100	67	117	83	91

tency estimates for the optical and electrical activities was 20 ms, well below the sampling rate for optical data (50 ms), $t(11) = -8.14$, $P < 0.0001$. In no case did the difference between the two estimates exceed 50 ms (which is the sampling rate for EROS). The average absolute difference was also smaller than the expected difference between the latency of the electrical activity peak and that of a random value for the EROS peak latency within the latency window considered for the analysis (50–150 ms), $t(11) = -4.77$, $P < 0.001$. It should also be noted, however, that although these data support the claim that the time courses of EROS and VEP activity share some common variance, they should not be taken as evidence that the two measures are caused by the same phenomena or by activation of the same area of the cortex. The increase in interelectrode variability may be due to activity outside of area 17 (or partly inside and partly outside), which may be temporally correlated with the activity observed in area 17 by using EROS.

The other approach to the comparison between the latency of the optical and electrical activities tests the hypothesis that the time course of EROS activity in area 17 should correspond, at least to some extent, with the time course of VEP activity from the same area. Since VEPs are surface measures, the time course of the VEP in area 17 needs to be estimated using a spatiotemporal dipole model (BESA algorithm described earlier in the paper). The time courses of the two responses (averaged across conditions) are overplotted in Fig. 6. To make the electrical data comparable with EROS (which were sampled using 50-ms bins), the estimated VEP activity from area 17 was averaged over periods of 50 ms. This figure indicates that the time course of the EROS response compared well with the modeled electrical activity. Note that, for each subject, the latencies of the positive and negative peaks of the EROS and VEP responses overlapped. This provides additional support for a temporal congruence of electrical and optical measures (at least within a 50-ms approximation).

DISCUSSION

The spatial correspondence between EROS and fMRI data and the temporal correspondence between EROS and VEP data validate the use of optical signals to study the time course of activity in localized cortical areas involved in processing visual stimuli. The spatial comparison shows the utility of coregistering EROS and fMRI data. Whereas fMRI data indicate that multiple cortical areas within the occipital region are activated by visual stimulation, the EROS data show that the time courses of activity in areas inside and outside area 17 (V1) are somewhat different. The EROS response in medial fMRI activation regions occurs before the EROS response in lateral fMRI activation areas. Further, the data indicate a substantial amount of spatial correspondence between the estimates of the localization of activity obtained with the two measures (the distance between the medial EROS and the fMRI foci is below 0.5 cm). There are two possible explanations for this distance. The first possibility is that it reflects the localization error of EROS. In this case, it is noteworthy to observe that the average distance between EROS and fMRI localization estimates is comparable to (and in fact smaller than) the sampling error of the optical data. Therefore, it is possible that a denser sampling of the occipital region with the optical measures could result in a smaller distance. The second possibility is that this distance is due to coregistration errors and/or to inherent differences in the localization of the physiological phenomena studied by the two measures. In this case, a finer spatial sampling of the occipital region with the optical measures would be of limited value. In any case, dense recording arrays are needed to determine the actual spatial resolution of noninvasive optical imaging. Tridimensional reconstruction algorithms can also be useful to increase spatial resolution and may provide estimates of the depth of the effect. However, application of dense recording arrays and tridimensional reconstruction algorithms can be practical only if parallel machines are built. At present, a 16-channel optical system capable of recording at sampling rates of at least 100 Hz is being tested.

The data also show a correlation between the timing

address this issue we have computed the correlations across subjects separately for each experimental condition and for the average across experimental conditions. All of these correlations are based on only three subjects. The correlations over subjects for each experimental condition ranged between 0.92 and 0.99 (the correlation could not be computed for the upper left quadrant stimulation condition since, for this condition, the latency of the optical response was 100 ms for all subjects—this was also the condition with smaller between-subject variability for the VEP response latency). The correlation based on the average estimates of the VEP and optical response latencies across conditions was 0.999 ($P < 0.05$).

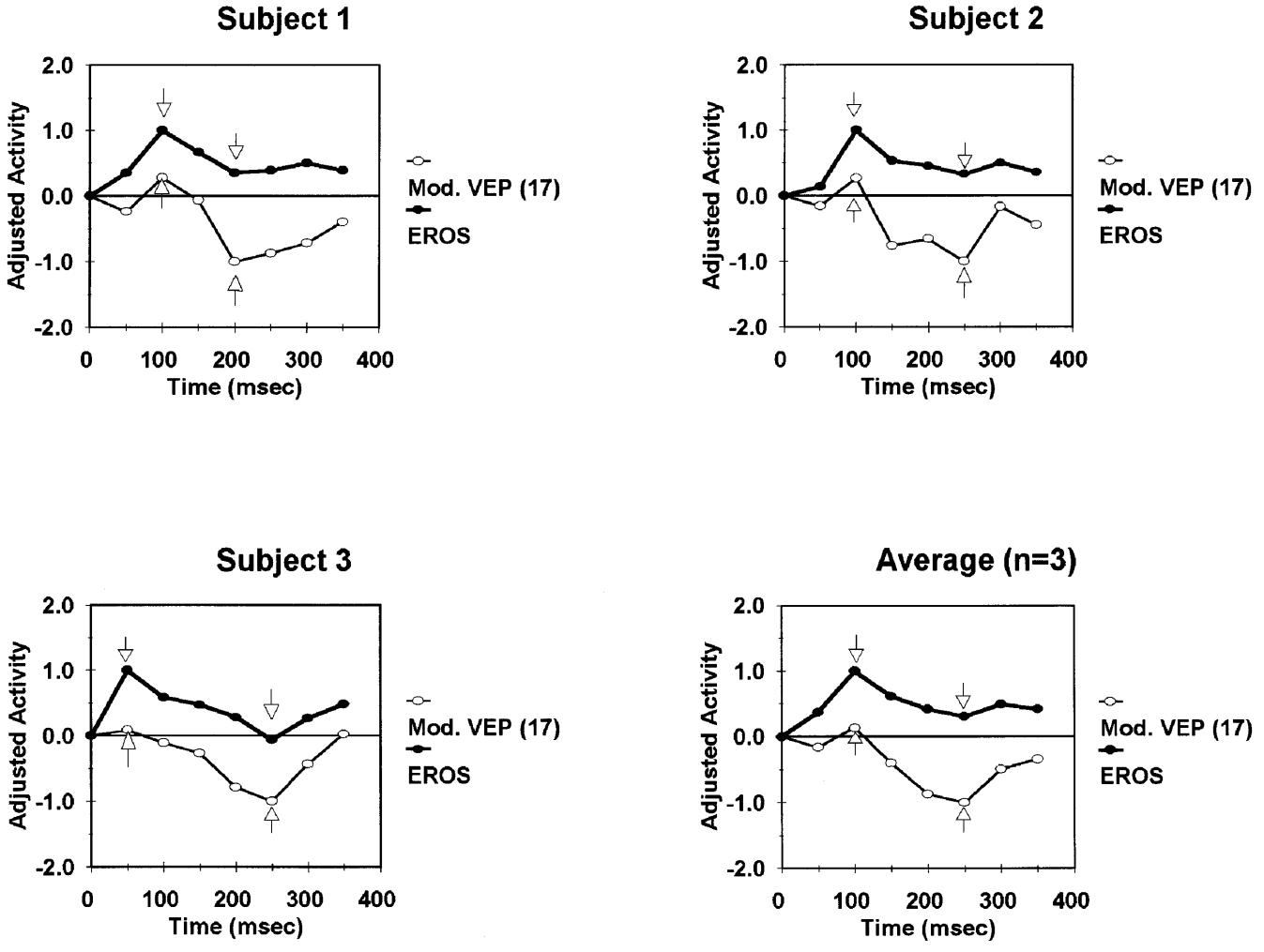

FIG. 6. Comparison of the time course of VEP[mod VEP(17)] and EROS from area 17. VEP is the estimated activity in area 17 obtained using a multiple spatiotemporal dipole model approach. EROS is the activity observed at the recording location with maximal increase in photon delay. For both measures, the data were averaged across conditions and are presented separately for each subject, with scales adjusted to make the results comparable (arbitrary units are used). For VEPs, upward deflections indicate that the positive pole of the modeled dipole source was oriented toward the surface of the head. For EROS, upward deflections indicate increases in photon delay. Arrows indicate peaks and troughs in the waveforms.

of EROS and the VEP activity. In the present study, both responses peak at a latency of approximately 100 ms after stimulation. In addition, conditions and subjects for which the EROS peaked earlier were also those for which the VEP responses were faster. Although these data support the use of optical measures to study the time course of brain activity, it should be clear that they do not imply that EROS and VEP responses are physical manifestations of the same phenomena. The VEP recorded using a particular scalp electrode pair is likely to be a much more complex phenomenon than the EROS response because it is the result of the summation of the electric fields generated in different (and sometimes distant) brain regions. For this reason, it is difficult to determine the time course of electrical activity in a selected brain area from surface evoked potentials. In this paper we approached this problem by modeling the surface electrical activity using pairs of dipoles located at some depth inside the head, one of which was considered to reflect activity in primary visual cortex—and therefore was considered to be the electrical counterpart of the localized activity measured with optical methods. The results of this modeling effort were mixed. On the one hand, the time courses of the electrical and optical activities were quite similar. On the other hand, the localization of the dipole source did not closely match that of EROS and fMRI activity, leaving doubts about whether the optical and electrical measures reflect activation of the same neuronal populations. Note, however, that the average distance between the sources and the foci of EROS and fMRI activity was comparable to the uncertainty of

localization inherent to the dipole modeling approach, as estimated by other authors (Miltner *et al.*, 1994).

The data reported in this paper help clarify the nature of EROS. The temporal agreement between optical and electrical measures suggests that they may share, at least in a very general sense, a common physiological mechanism. Since surface electrical measures are believed to be direct indices of neuronal activity (Nunez, 1981), it is plausible that noninvasive optical measures may also reflect neuronal activity directly. Neuronal activity is associated with movement of ions across and around the neuronal membrane, which results in the surface electrical response (Nunez, 1981) and in changes in the osmolar and refractive properties of intra- and extracellular compartments. These, in turn, may influence the scattering properties of the medium (Cohen, 1972; Hill and Keynes, 1949; Stepnowski *et al.*, 1991). However, more research is needed to determine the specific physiological phenomena that are visualized using EROS.

Because of its complex nature, the present study was conducted on a relatively small number of subjects ($N = 3$). However, three more studies have been recently completed in which an EROS response from medial occipital areas (presumably area 17) with a latency of approximately 100 ms from visual stimulation was observed (Gratton, 1997; Gratton *et al.*, submitted for publication; Goodman *et al.*, 1996). In each of these studies, all subjects show an early medial occipital optical response. These findings indicate that an early response from area 17 can be reliably detected with EROS.

The temporal correspondence between EROS and VEP suggests that EROS is more likely to be an index of neuronal activity than a measure of the subsequent vascular response (measured using fMRI). However, the data also point to a spatial correspondence between EROS and fMRI. Recently, there has been some discussion about the extent to which the vascular responses measured by the fMRI-BOLD signal colocalize with the neuronal response. Recent work by Malonek and Grinvald (1996), based on optical measurements taken on the exposed cortex, indicates that the increased oxygenation of the cortex, which is the basis of the BOLD-fMRI, occurs after 2 s from stimulation in an area that is a few millimeters wider than the area where the initial neuronal response is observed. They also observed a faster deoxygenation response and rapid scattering effects with an even more accurate localization. In our study, the average distance between EROS and fMRI localization is also a few millimeters. Thus the data from the present study are consistent with the interpretation that the early EROS phenomenon observed is directly related to the neuronal response. An alternative account for the early EROS response is that it is related to some other early phenomenon within the cascade between the neuronal and the vascular phenomena (e.g., the diffusion of some chemical mediator).

The temporal correspondence between optical and electrical data and the spatial congruence of optical and hemodynamic measures provide a systematic approach to integrating various brain imaging methods, opening the possibility for an enhanced spatiotemporal description of brain activity.[7] Both fMRI and electrical data reveal the existence of multiple responses (at different locations and at different times, respectively). In relating these two sets of data, it is important to determine which of the spatial structures identified using fMRI corresponds to which temporal aspect of the electrophysiological signal. The data reported in this paper suggest that EROS can be particularly useful in addressing this question. For this reason, EROS may be ideally suited for studying the dynamic interactions of different brain areas which are likely to underlie most higher brain functions (Mesulam, 1990; Squire, 1989).

ACKNOWLEDGMENTS

This work was supported in part by Grants MH57125 from NIMH to Dr. Gabriele Gratton, EY02115 from the NEI to Dr. Donald Hood, AG05213 from NIA to Dr. David Friedman, CA57032 from NIH to Dr. Enrico Gratton, the Center for Functional Imaging at the MSKCC (Dr. Joy Hirsch, Director), and the William T. Morris Foundation Fellowship to Karl Kim. We thank Victoria Kasmerski, M. Catherine DeSoto, and two anonymous reviewers for comments on an earlier version of the manuscript, and we thank Eunhee Cho for helping with data collection.

[7] See Heinze *et al.* (1994) for an example of another approach to integrating hemodynamic and electrophysiological data.

REFERENCES

Cannestra, A. F., Blood, A. J., Black, K. L., and Toga, A. W. 1996. The evolution of optical signals in human and rodent cortex. *Neuroimage* **3:**202–208.

Chance, B. 1988. Multi-element phase arrays for phase modulation imaging. *Proc. SPIE* **1888:**354–358.

Chance, B., Kang, K., He, L., Weng, J., and Sevick, E. 1993a. Highly sensitive object location in tissue models with linear in-phase and anti-phase multi-element optical arrays in one and two dimensions. *Proc. Natl. Acad. Sci. USA* **90:**3423–3427.

Chance, B., Zhuang, Z., UnAh, C., Alter, C., and Lipton, L. 1993b. Cognition-activated low-frequency modulation of light absorption in human brain. *Proc. Natl. Acad. Sci. USA* **90:**3770–3774.

Churchland, P. S., and Sejnowski, T. J. 1988. Perspectives in cognitive neuroscience. *Science* **242:**741–745.

Clark, V. P., and Hillyard, S. A. 1996. Spatial selective attention affects early extrastriate but not striate components of the visual evoked potential. *J. Cogn. Neurosci.* **8:**377–402.

Cohen, L. B. 1972. Changes in neuron structure during action potential propagation and synaptic transmission. *Physiol. Rev.* **53:**373– 417.

Delpy, D. T., Cope, M., van der Zee, P., Arridge, S., Wray, S., and Wyatt, J. 1988. Estimation of optical pathlength through tissue from direct time-of-flight measurements. *Phys. Med. Biol.* **33:**1433–1442.

Fishkin, J. B., and Gratton, E. 1993. Propagation of photon-density waves in strongly scattering media containing an absorbing semi-infinite plane bounded by a straight edge. *J. Opt. Soc. Am.* **A10:** 127–140.

Frostig, R. D., Lieke, E. E., Ts'o, D. Y., and Grinvald, A. 1990. Cortical functional architecture and local coupling between neuronal activity and the microcirculation revealed by in vivo high-resolution optical imaging of intrinsic signals. *Proc. Natl. Acad. Sci. USA* **87:**6082–6086.

Goodman, M. R., Bauer, R. M., Corballis, P. M., Hood, D. C., and Gratton, G. 1996. Human optical signals and visual evoked potentials (VEPs) from different cone systems. *Invest. Ophtalmol. Vis. Sci.* **37:**S708.

Gratton, E., and Limkeman, M. 1983. A continuously variable frequency cross-correlation phase fluorometer with picoseconds resolution. *Biophys. J.* **44:**315–324.

Gratton, E., Jameson, D. M., Rosato, N., and Weber, G. 1984. Multifrequency cross-correlation phase fluorometer using synchrotron radiation. *Rev. Sci. Instr.* **55:**486–493.

Gratton, G. 1997. Attention and probability effects in the human occipital cortex: An optical imaging study. *NeuroReport,* **8:**1749–1753.

Gratton, G., Coles, M. G. H., and Donchin, E. 1983. A new method for off-line removal of ocular artifact. *Electrophysiol. Clin. Neurophysiol.* **55:**468–484.

Gratton, G., and Corballis, P. M. 1995. Removing the heart from the brain: Compensation for the pulse artifact in photon migration signal. *Psychophysiology* **32:**292–299.

Gratton, G., Corballis, P. M., Cho, E., Fabiani, M., and Hood, D. C. 1995a. Shades of gray matter: Non-invasive optical images of human brain responses during visual stimulation. *Psychophysiology* **32:**505–509.

Gratton, G., Fabiani, M., Friedman, D., Franceschini, M. A., Fantini, S., Corballis, P., and Gratton, E. 1995b. Rapid changes of optical parameters in the human brain during a tapping task. *J. Cogn. Neurosci.* **7:**446–456.

Gratton, G., Fabiani, M., Goodman-Wood, M. R., and DeSoto, M. C. Memory effects in human primary visual cortex: Evidence from the event-related optical signal (EROS). [Submitted for publication].

Grinvald, A., Lieke, E., Frostig, R. D., Gilbert, C. D., and Wiesel, T. N. 1986. Functional architecture of cortex revealed by optical imaging of intrinsic signals. *Nature* **324:**361–364.

Haglund, M. M., Ojemann, G. A., and Hochman, D. W. 1992. Optical imaging of epileptiform and functional activity in human cerebral cortex. *Nature* **358:**668–671.

Heinze, H. J., Mangun, G. R., Burchert, W., Hinrichs, H., Scholz, M., Munte, T. F., Gos, A., Scherg, M., Johannes, S., Hundeshagen, H., Gazzaniga, M. S., and Hillyard, S. A. 1994. Combined spatial and temporal imaging of brain activity during visual selective attention in humans. *Nature* **372:**543–546.

Hill, D. K., and Keynes, R. D. 1949. Opacity changes in stimulated nerve. *J. Physiol.* **108:**278–281.

Hirsch, J., DeLaPaz, R. L., Relkin, N., Victor, J., Kim, K., Li, T., Borden, P., Rubin, N., and Shapley, R. 1995. Illusory contours activate specific regions in human visual cortex: Evidence from functional magnetic resonance imaging. *Proc. Natl. Acad. Sci. USA* **92**(July):6469–6473.

Hoshi, Y., and Tamura, M. 1993. Dynamic multichannel near-infrared optical imaging of human brain activity. *J. Appl. Physiol.* **75:**1842–1846.

Kato, T., Kamei, A., Takashima, S., and Ozaki, T. 1993. Human visual cortical function during photic stimulation monitored by means of near-infrared spectroscopy. *J. Cereb. Blood Flow Metab.* **13:**516–520.

Maier, J., Dagnelie, G., Spekreijse, H., and van Dijk, B. W. 1987. Principal components analysis for source localization of VEPs in man. *Vision Res.* **27:**165–177.

Malonek, D., and Grinvald, A. 1996. Interactions between electrical activity and cortical microcirculation revealed by imaging spectroscopy: Implications for functional brain mapping. *Science* **272:**551–554.

Meek, J. H., Elwell, C. E., Khan, M. J., Romaya, J., Wyatt, J. S., Delpy, D. T., and Zeki, S. 1995. Regional changes in cerebral hemodynamics as a result of a visual stimulus measured by near infrared spectroscopy. *Proc. R. Soc. London Ser. B Biol. Sci.* **261:**351–356.

Mesulam, M. M. 1990. Large-scale neurocognitive networks and distributed processing for attention, language, and memory. *Ann. Neurol.* **24:**439–445.

Miltner, W., Braun, C., Johnson, R., Jr., Simpson, G. V., and Ruchkin, D. S. 1994. A test of brain electrical source analysis (BESA): A simulation study. *Electroencephalogr. Clin. Neurophysiol.* **91:**295–310.

Nunez, P. L. 1981. *Electric Fields of the Brain.* Oxford, New York.

Scherg, M., Vajsar, J., and Picton, T. W. 1989. A source analysis of the human auditory evoked potentials. *J. Cogn. Neurosci.* **1:**336–355.

Squire, L. R. 1989. Mechanisms of memory. In *Molecules to Models: Advances in Neuroscience* (K. L. Kelner and D. E. Koshland, Eds.), AAAS, Washington, DC.

Stepnowski, R. A., LaPorta, J. A., Raccuia-Behling, F., Blonder, G. E., Slusher, R. E., and Kleinfeld, D. 1991. Noninvasive detection of changes in membrane potential in cultured neurons by light scattering. *Proc. Natl. Acad. Sci. USA* **88**(November):9382–9386.

Toga, A. W., and Mazziotta, J. C. 1996. *Brain Mapping: The Methods.* Academic Press, San Diego.

Villringer, A., Planck, J., Hoch, C., Schleinkofer, L., and Dirnagl, U. 1993. Near infrared spectroscopy (NIRS): A new tool to study hemodynamic changes during activation of brain function in human adults. *Neurosci. Lett.* **154:**101–104.